APPLIED GEOPHYSICS, Vol.13, No.1 (March 2016), P. 48-58, 17 Figures.
DOI:10.1007/s11770-016-0534-4

Research on RTP aeromagnetic gradient data and its applicability in different latitudes*

Li Lin[1], Guo Hua[♦2,3], Wang Ping[2,3], and Jia Wei-Jie[3]

Abstract: Aeromagnetic gradient data needs to be reduced to the pole so that it can be better applied to geological interpretation through theoretical derivation. In this paper, we conduct research on the morphological characteristics of the total and horizontal gradient modules before and after reduction to the pole and design models at different latitudes, with consistent and inconsistent magnetic field direction and geological body magnetization direction. We discuss how to use the total gradient module and horizontal gradient module in geological interpretation. The reduced-to-the-pole (RTP) method is required for the horizontal gradient module method but not for the total gradient module. Finally, the conclusions derived from the theoretical models are verified through analysis of real data. The position determination of a geological body using the total gradient method, gradient data, or total-field data works better without RTP, ensuring data primitive authenticity. However, the horizontal gradient module should be reduced to the pole to determine the boundary of the geological body. Finally, the correction of the designed model is verified by actual data analysis. Both the total and horizontal gradient methods can be applied to geological interpretation.
Keywords: Aeromagnetic gradient data, reduction to the pole, total gradient module, horizontal gradient module

Introduction

Airborne magnetic data is generally reduced to the pole (RTP) or to the equator before geological interpretation, especially when delineating the boundaries of a rock body. Such data and the resulting gradient data are necessary to correlate the maximum number of anomalous data points from the airborne magnetic data with the central position of the geological body, and thus better represent its boundaries. However, it is currently uncertain whether similar RTP application is necessary for measured gradient data when they are used for geological interpretation. Few scholars believe that gradient data are superior to ΔT data for filtering anomalies and for delineating geological boundaries in geological interpretation (Peter, 1986; Wang and Sun, 1990; Guan et al., 1996; Zhang, 2006; Li and Chang, 2009; Xian et al., 2013). However, while directly attempting to delineate the boundaries of rock bodies using vertically measured gradient data, we discovered that the resulting geological boundaries shifted

Manuscript received by the Editor August 3, 2015; revised manuscript received February 24, 2016.
*This paper is surpported by the National 863 Program (Grant No. 2013AA063901).
1. College of Geo-exploration Sciences and Technology, ilin University, Chang Chun 130026, China,
2. China University of Geosciences (Beijing), Beijing 100083, China,
3. China Aero Geophysical Survey and Remote Sensing Center, Beijing 100083, China.
♦Corresponding author, Guo Hua (Email: hyguohua@126.com)

southwards relative to those determined using the total field. Therefore, applications such as total-field RTP need to be applied to gradient data before geological interpretation.

Reduction to the pole (or equator) can remove the influence of obliquely biased magnetization and precisely determine geological boundaries. This theory was first put forward by Baranov in 1957. In a further study, Ervin (1976) used FFT to perform RTP, improving efficiency. At low latitudes, the RTP factor is perpendicular to the geomagnetic dip direction due to an instability. Baranov limited the magnetic inclination of the RTP algorithm to 16.5° (Baranov and Naudy, 1964), then Silva corrected it to 15° (Silva, 1986). Hansen and Pawlowski (1989) used the Wiener filter to perform RTP, applying it to low latitude areas. Later, Blakely used reduction to the equator to replace the RTP process, but the application is limited as processing the horizontal magnetic data is difficult (Blakely, 1996). Some modified numerical computation methods, such as analytical signal representation and a frequency conversion two-way damping factor method, further improved the calculation speed of RTP. These more effectively extract the geological feature information and improve the applicability in low latitude areas (Keating and Zerbo, 1996; Ansari and Alamdar, 2009; Lin and Ping, 2012; Baranov and Naudy, 1964). However, studies on the magnetic data RTP process exist only for total-field and converted gradient data. For the geological interpretation measured gradient data has obvious advantages relative to total field data while compiling anomalies and delineation of geological boundaries (Peter, 1986; Pedersen and Rasmussen, 1990; Godio and Piro, 2005; Zhang, 2006; Li and Chang, 2009; Xian et al., 2013). Through theoretical derivation and systematic analysis of measured vertical gradient data, the author suggests that the measured gradient data should be processed by RTP before geological interpretation can take place.

The total gradient module method for magnetic anomalies was first used for the interpretation of 2D magnetic profile data (Nabighian, 1972). The method has become a geophysical inversion hotspot over several decades of development. Directed at the top surface of a slanting clintheriform body, Guan and Yao (1997) introduced the gradient module inverse method, which can invert parameters such as inclination and width. Huang and Guan (1998) analyzed the relation between the total gradient module magnetic anomaly maximum value and the position of the magnetic source boundary and obtained good feedback. Regarding aeromagnetic data, Guo et al. (2004) stated that one important function of the total (or horizontal) gradient module method is a delineation of the horizontal geological structure boundary. Wu et al. (2013) put forward the use of the total gradient module method for low latitude areas. Some scholars discuss the horizontal total gradient module method, assuming that the density or magnetism of a geological body has a single vertical boundary, the boundary position can be determined using the maximum value position of the horizontal total gradient module map (Li and Yang, 2009; Liu et al., 2006; Qi et al., 2009). However, no attention has yet been paid to the total or horizontal gradient modules at different latitudes.

In this study, we present the total and horizontal gradient module methods at different latitudes using theoretical derivation and model analysis. This paper also discusses geological interpretation in post-processing and the actual effects of the total and horizontal gradient modules, providing a foundation for the application of gradient data to geologic interpretation.

Theory of gradient-reduction-to-the-pole (GRTP) and the magnetic anomaly module

Derivation of the theoretical formula for gradient RTP

Before use in geological interpretation, total intensity magnetic anomalies are reduced to the pole to remove asymmetries induced by the declination of the magnetic field. This process simplifies the morphology of the anomalies and facilitates interpretation. The theoretical calculation of the total magnetic intensity anomaly RTP is expressed as equation (1) (Gunn, 1975).

$$\tilde{\Delta Z}_{\perp} = \frac{u^2+v^2}{[i(lu+mv)+n\sqrt[2]{u^2+v^2}]^2}\tilde{\Delta T}, \tag{1}$$

where u and v are the circular frequencies in the x and y directions, $r=\sqrt{u^2+v^2}$; l, m, and n are the directional cosines in the magnetization direction, $l=\cos I\cos D$, $m=\cos I\sin D$ and $n=\sin I$. In this equation, I is the inclination of the geomagnetic field, D is the declination of the geomagnetic field, and $\tilde{\Delta T}$ is the measured ΔT spectrum of ΔT.

To derive the theoretical RTP formula for gradient data, a theoretical calculation formula is needed for the spectrum of the measured first-order vertical and horizontal derivatives of the total field.

From the expressions of the field and spectra, the first-order vertical derivative and its spectrum is (Sun et al., 1995)

$$\frac{\partial \tilde{F}}{\partial z} = -\frac{\partial \tilde{F}}{\partial \mathrm{h}} = r\tilde{F}. \quad (2)$$

Using a differential Fourier transform, the spectrum of the first-order horizontal derivative is

$$\frac{\partial \tilde{F}}{\partial x} = iu\tilde{F}, \quad (3)$$

$$\frac{\partial \tilde{F}}{\partial y} = iv\tilde{F}. \quad (4)$$

The above formulae provide the fundamental theoretical prerequisite for derivation of measured gradient data for further processing. The calculation factors required for deriving measured vertical and horizontal gradients can be obtained using these theoretical formulae. The theoretical formula for gradient RTP is derived from known formulae as shown below:

From equation (1), we obtain:

$$\frac{\partial \widetilde{\Delta Z_{\perp}}}{\partial x} = \frac{u^2+v^2}{[i(lu+mv)+n\sqrt[2]{u^2+v^2}]^2}\frac{\partial \widetilde{\Delta T}}{\partial x}, \quad (5)$$

$$\frac{\partial \widetilde{\Delta Z_{\perp}}}{\partial y} = \frac{u^2+v^2}{[i(lu+mv)+n\sqrt[2]{u^2+v^2}]^2}\frac{\partial \widetilde{\Delta T}}{\partial y}, \quad (6)$$

$$\frac{\partial \widetilde{\Delta Z_{\perp}}}{\partial z} = \frac{u^2+v^2}{[i(lu+mv)+n\sqrt[2]{u^2+v^2}]^2}\frac{\partial \widetilde{\Delta T}}{\partial z}, \quad (7)$$

where As $\widetilde{\Delta Z_{\perp}}$ can be assumed to be the total-field magnetic anomaly collected at the pole, equations (5), (6), and (7) can be transformed into:

$$iu\widetilde{\Delta Z_{\perp}} = \frac{u^2+v^2}{[i(lu+mv)+n\sqrt[2]{u^2+v^2}]^2}iu\widetilde{\Delta T}, \quad (8)$$

$$iv\widetilde{\Delta Z_{\perp}} = \frac{u^2+v^2}{[i(lu+mv)+n\sqrt[2]{u^2+v^2}]^2}iv\widetilde{\Delta T}, \quad (9)$$

$$r\widetilde{\Delta Z_{\perp}} = \frac{u^2+v^2}{[i(lu+mv)+n\sqrt[2]{u^2+v^2}]^2}r\widetilde{\Delta T}. \quad (10)$$

From equations (8), (9), and (10), all gradient data, whether traverse, longitudinal or vertical, can eventually be transformed into equation (1). That is, treatment similar to total-field RTP is also required for gradient data before the resulting contour line corresponds to the boundaries of a geological body.

Magnetic anomaly total gradient module

The magnetic anomaly total gradient module is (Nabighian, 1972):

$$\Delta T_G = (\Delta T_x^2 + \Delta T_y^2 + \Delta T_z^2)^{1/2}, \quad (11)$$

where ΔT_x, ΔT_y, ΔT_z are two horizon gradient components and vertical gradient components of ΔT. For a two-dimensional body, the magnetic anomaly total gradient module is as follows:

$$\Delta T_G = (\Delta T_x^2 + \Delta T_z^2)^{1/2}. \quad (12)$$

The horizontal gradient module of the magnetic anomaly is:

$$\Delta T_{\mathrm{xy}} = (\Delta T_x^2 + \Delta T_y^2)^{1/2}. \quad (13)$$

According to the formula of an arbitrary cross-sectional inhomogeneous magnetized two-dimensional body magnetic anomaly, there is no connection between ΔT_G and the magnetization direction (Guan et al., 1993). But for a three-dimensional body, the shape is uniform between the different magnetization directions of ΔT_G. This shows that ΔT_G is affected by the magnetization direction, but its influence is smaller than that of the total magnetic anomaly.

Model testing

Performing RTP on gradient data transforms the data collected from different latitudes so that the values are the same as if the data had been collected at the pole. The data are then more useful for delineating geological body boundaries and determining the central positions of deep geological bodies. Subsequent geological interpretation becomes easier after treatment with methods such as the total gradient module and the horizontal gradient module. However, the regular characteristics of the gradient module contour map or ΔT data at different latitudes needs more discussion. For this purpose, some theoretical models were designed to determine the effects and characteristics of gradient data after RTP and some conclusions reached may serve as a basis for future geological interpretation. Before model testing, the gradient data from theoretical calculations were equalized to the airborne magnetic gradient data from actual measurements, i.e., the measured gradient data.

To allow a more effective interpretation of the distribution of underground geological bodies, we designed models that displayed consistent and inconsistent magnetic field directions and magnetization directions. We used the total gradient module contour map of the gradient data, the total-field data, and the horizontal gradient module of the gradient data to analysis the influence of RTP on each of them. The purpose of this model was to find out how different the contour maps produced were, and what should be taken into account when using them for interpretation.

Theoretical model with uniform magnetization direction

Model parameters as shown in Table 1:

Table 1 The model parameters

Model number	Direction of magnetic field		Direction of magnetization		Width (m)	Length (m)	Depth to top (m)	Depth to bottom (m)	Intensity of magnetization (A /M)
	I (°)	*D* (°)	*I* (°)	*D* (°)					
1	0, 20, 30, 40, 60	-6	0, 20, 30, 40, 60	-6	1500	1500	1000	2500	10
2	0, 20, 30, 40, 60	-6	0, 20, 30, 40, 60	-6	400	400	200	600	10
3	0, 20, 30, 40, 60	-6	0, 20, 30, 40, 60	-6	400	400	500	900	20
4	0, 20, 30, 40, 60	-6	0, 20, 30, 40, 60	-6	200	200	100	300	20

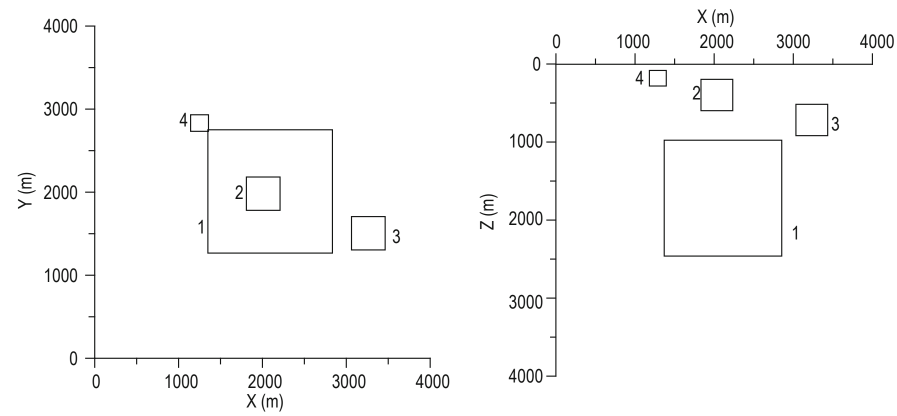

Fig.1 XY plane and XZ plane profiles of the theoretical model.

First, analysis of the contour map of the total gradient modules of the gradient data before and after RTP can be seen in Figures 2 and 3. Figures 2a, 2b, 2c, 2d, and 2e show the total gradient module of the gradient data before RTP with magnetization dip angles I = 0°, 20°, 30°, 40°, and 60°, respectively. The red rectangles represent the projection of a geological body in the plane XY. It can be seen from the figure that the maximum position of the total gradient module of the gradient data before RTP and the center of geological body did not fully correspond. When I = 20°, the position of the maximum contour of the total gradient module is in the XY plane projection range, but compared to the position of the center it is off to the north. When I = 30°, 40°, and 60°, the position of the maximum contour of the total gradient module is in the XY plane projection range, but compared to the position of the center it is off to the south. And when I = 0°, the maximum value position corresponds to the center position of the geological body. When I = 20° and 30°, the influence of the background field is obvious on the contour map of total gradient module; it is the false anomaly in the north of model 1. In the total gradient module contour map of gradient data after RTP (Figure 3), the maxima represent the center positions of models 2, 3, and 4 and the marginal anomaly produced by model 1 does not appear. The contour map shape of the total gradient module after RTP is closer to the model body form than with no RTP.

RTP aeromagnetic gradient data

It is worth noting that when $I = 0°$, the shape of anomaly before RTP is tidier than after. Figures 4 and 5 show the correspondence of the total gradient module contour map with geological body after RTP and derivation. Like the gradient data calculation, the correspondence of the total gradient module contour map maxima with model's center position is better after RTP and derivation. After analysis it can be seen that the reflection of the anomaly in the north of model 1 is stronger in Figure 4 than in Figure 2. In addition, when $I = 20°$, $30°$, and $40°$, the boundary effect occurs in the eastern part of the surveyed area, before RTP and derivation of total-field data. This is mainly a result of the derivation process and it also influence the data after RTP and derivation. However, the gradient data show no boundary effects. After analysis of Figures 3 and 5 we can see that when $I = 0°$,

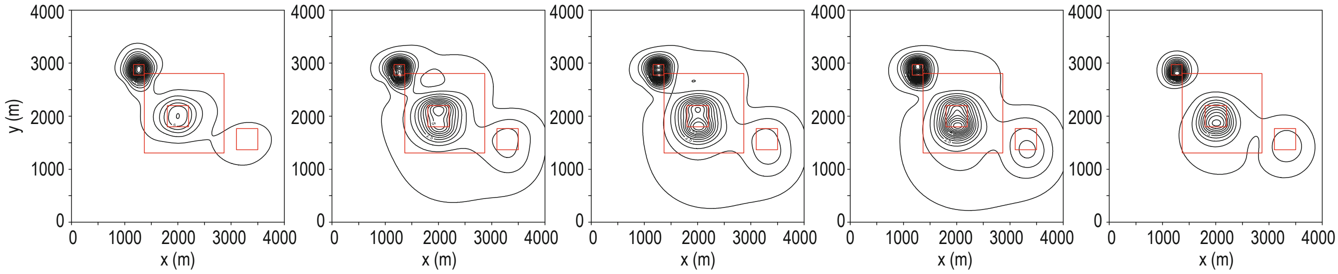

(a) $I = 0°$ (b) $I = 20°$ (c) $I = 30°$ (d) $I = 40°$ (e) $I = 60°$

Fig.2 Contours of total gradient module of gradient data before RTP.

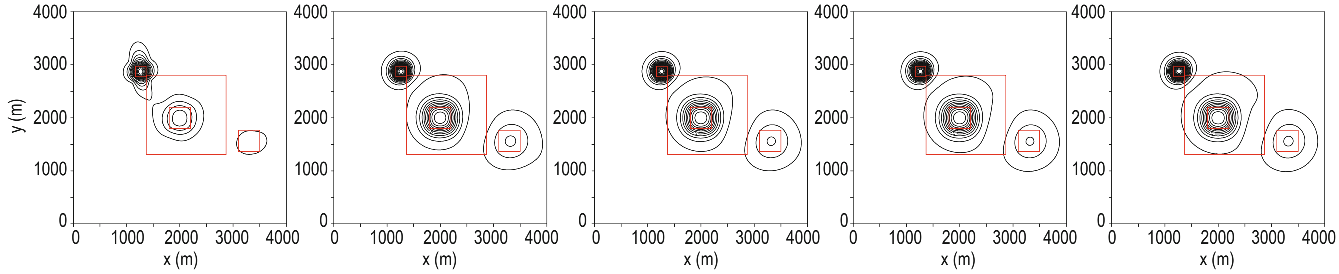

(a) $I = 0°$ (b) $I = 20°$ (c) $I = 30°$ (d) $I = 40°$ (e) $I = 60°$

Fig.3 Contours of total gradient module of gradient data after RTP.

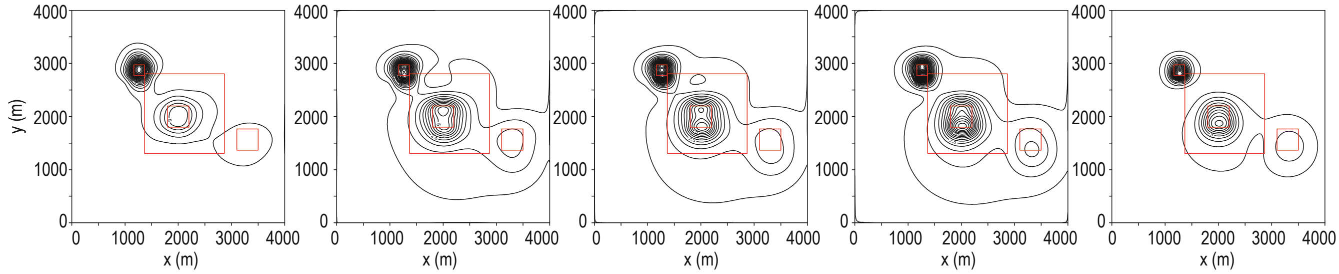

(a) $I = 0°$ (b) $I = 20°$ (c) $I = 30°$ (d) $I = 40°$ (e) $I = 60°$

Fig.4 Contours of total gradient module of total-field data derivation before RTP.

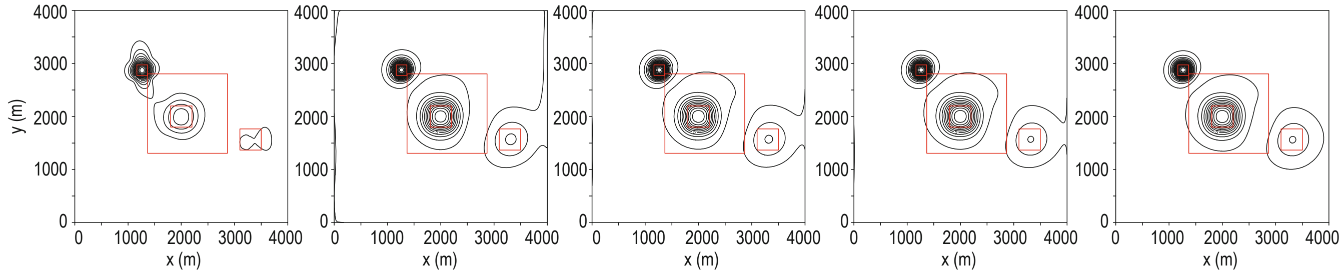

(a) $I = 0°$ (b) $I = 20°$ (c) $I = 30°$ (d) $I = 40°$ (e) $I = 60°$

Fig.5 Contours of total gradient module of total-field data derivation after RTP.

the shape of the total gradient module contour map has obviously changed. The boundary effect also occurred in the eastern part of the surveyed area after RTP and derivation for the same reason.

When the magnetic field direction is consistent with the geological magnetization direction, the conclusion is as follows: First, due to the influence of the background field, the RTP process works well for determining the boundary of the geological body using the total gradient module method for gradient data and total-field data. Second, the boundary effect of the total-field data should be noted when I = 20°–40°. Third, the background field is not obvious on the total gradient module contour map.

The reflection effect of the boundary in the horizontal gradient module method needs further analysis. For I = 40°, Figure 6 is the horizontal gradient module contour map of gradient data before RTP and Figure 7 is the map after RTP. Figure 6 shows that the maxima of the horizontal gradient module before RTP did not reflect the model's boundary position accurately. As can be seen from Figure 7, the boundary and center position of models 2 and 4 correspond well to the maxima of the horizontal gradient module. Meanwhile, it is influenced by the background interference produced from model 1. Due to the burial depth, model 3 is deeper than models 2 and 4, and the horizontal gradient module method does not reflect the center and boundary positions, and produces some interference in the east of model 1. Conclusions: firstly, the horizontal gradient module, obtained after RTP of gradient data, better reflects the center position and the boundary for the shallower parts of the model, and the effect of a deep anomaly is not obvious; secondly, the reflection of the background field in the horizontal gradient module is not obvious.

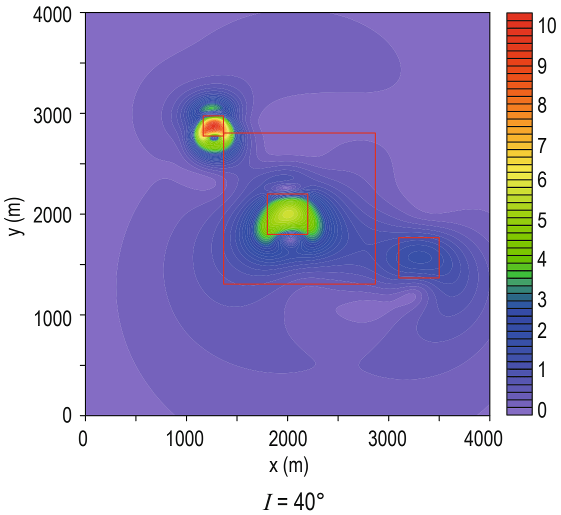

Fig.6 Contours of horizontal gradient module of gradient data before RTP.

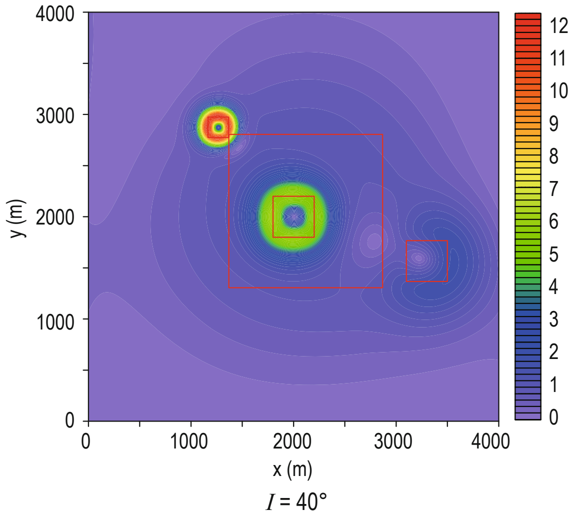

Fig.7 Contours of horizontal gradient module of gradient data after RTP.

Theoretical models with different magnetization directions

For complex geological bodies where the magnetization direction is inconsistent, a contour map of gradient data treated with RTP and total-field data treated with RTP and derivation, is discussed.

Model parameters as shown in Table 2:

Table 2 The model parameters

Model number	Direction of magnetic field		Direction of magnetization		Width (m)	Length (m)	Depth to top (m)	Depth to bottom (m)	Intensity of magnetization (A /M)
	I (°)	D (°)	I (°)	D (°)					
1	0, 20, 30, 40, 60	-6	70	-6	1500	1500	1000	2500	10
2	0, 20, 30, 40, 60	-6	20	-6	400	400	200	600	10
3	0, 20, 30, 40, 60	-6	50	-6	400	400	500	900	20
4	0, 20, 30, 40, 60	-6	10	-6	200	200	100	300	20

RTP aeromagnetic gradient data

From Figures 8 and 10 it can be seen that when I > 20°, the position of the maximum contour of the total gradient module compared to the position of the center is south of the model's real position, co nsistent with the above conclusion. When 0 < I < 20°, it is north of model's real position and when I = 0°, the position of maximum value corresponds to the center of the geological body. Whatever magnetic inclination, the position of the maximum contour of the total gradient module is in the projection range of the XY plane. When I = 0° or 60°, the north of the model 1 shows some interference. Figures 8 and 10 show that for the same inclination of magnetic field, the total gradient module contour map of the gradient data and field data before

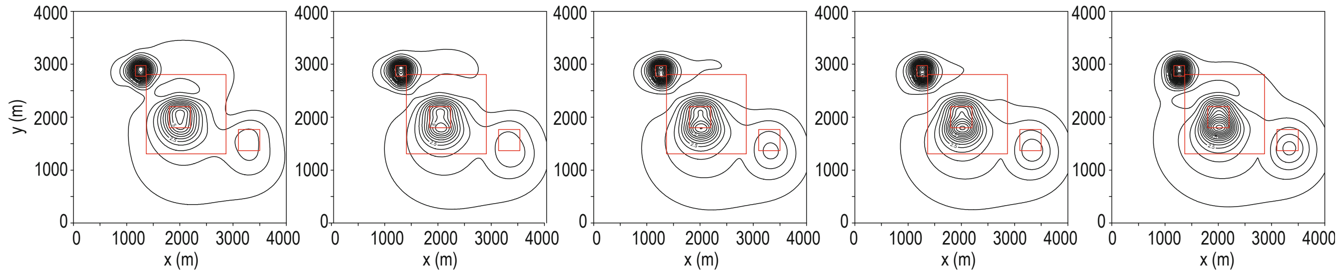

(a) I = 0° (b) I = 20° (c) I = 30° (d) I = 40° (e) I = 60°

Fig.8 Contours of total gradient module of gradient data before RTP.

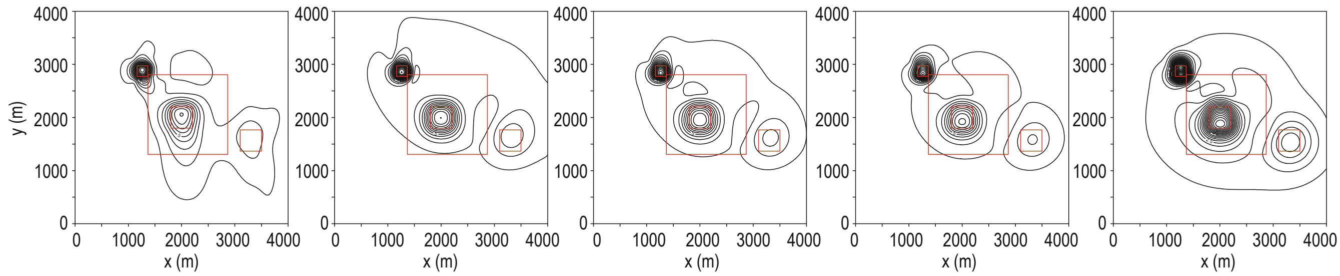

(a) I = 0° (b) I = 20° (c) I = 30° (d) I = 40° (e) I = 60°

Fig.9 Contours of total gradient module of gradient data after RTP.

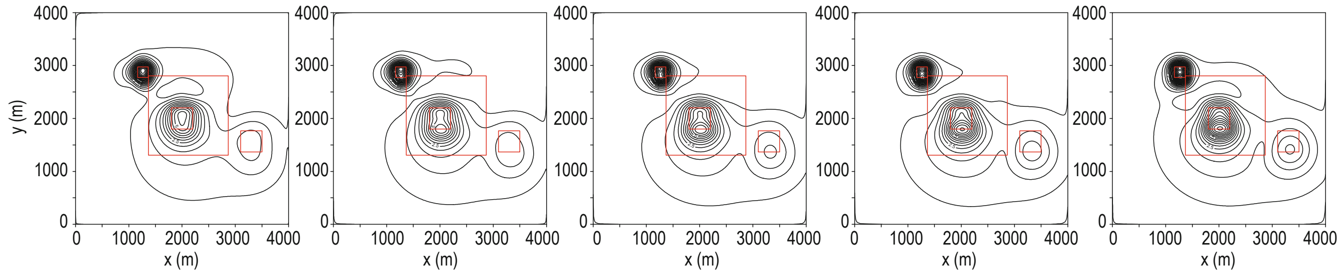

(a) I = 0° (b) I = 20° (c) I = 30° (d) I = 40° (e) I = 60°

Fig.10 Contours of total gradient module of total-field data derivation before RTP.

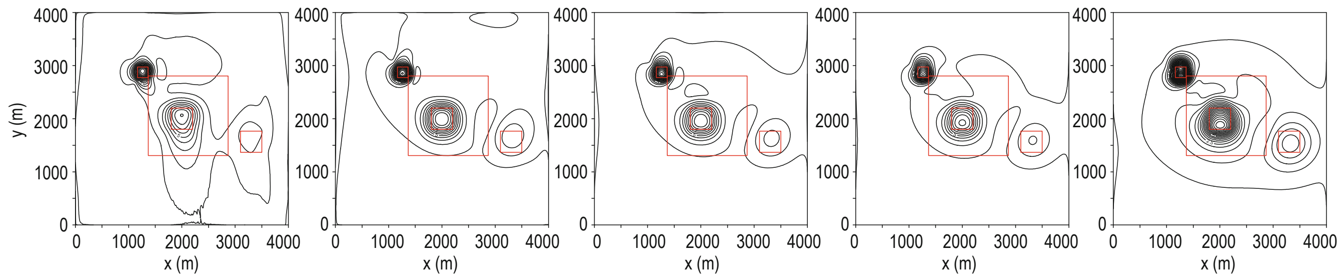

(a) I = 0° (b) I = 20° (c) I = 30° (d) I = 40° (e) I = 60°

Fig.11 Contours of total gradient module of total-field data derivation after RTP.

RTP and derivation are basically the same. However, in Figure 10, a boundary effect appears in the east of the contour map of total gradient modules. This is because of the process of derivation in the frequency domain. Figures 9 and 11 are contour maps of the gradient data and the total gradient module of field data treated with RTP and derivation. The offset direction of the anomalous body center is influenced by two factors: the geomagnetic inclination and the magnetization direction. It can be seen from Figures 9 and 10 that compared with the contour map of the total gradient modules before RTP, instead of simplify the anomaly morphology there is more interference, which hinders the geological interpretation. We draw the conclusion that when using the total gradient module for geological interpretation the RTP process is not needed, but the total gradient module cannot be applied to determine the boundary.

Illustrating the inconsistency of geomagnetic inclination and magnetization direction, Figure 12 is a contour map of the total gradient module of the gradient data before RTP and Figure 13 is the contour map after RTP. It can be seen from the figures that the effect of RTP is obvious. The shape of anomaly is more regular and its center position and boundary are more accurate. We therefore draw the conclusion that when applying the horizontal gradient module geological boundary analysis, the RTP process is needed.

Due to the complexity of geological bodies, the geomagnetic inclination and magnetization direction is always inconsistent. According to the above analysis, it is suggested that to determine the boundary and center position of geological body, the total gradient module of the gradient data before RTP and the horizontal gradient module after RTP should be used.

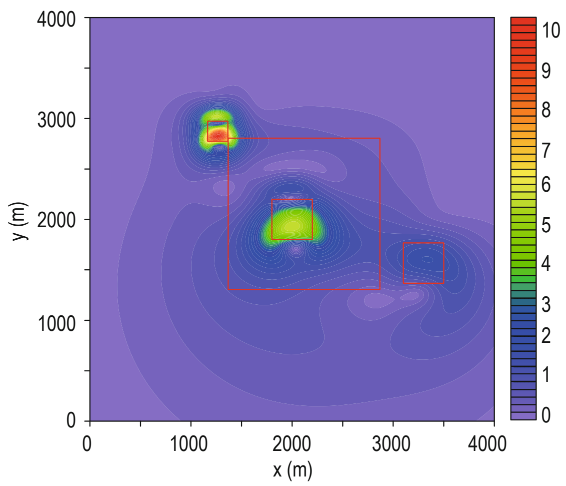

Fig.12 Contours of horizontal gradient module of gradient data before RTP at I = 40°.

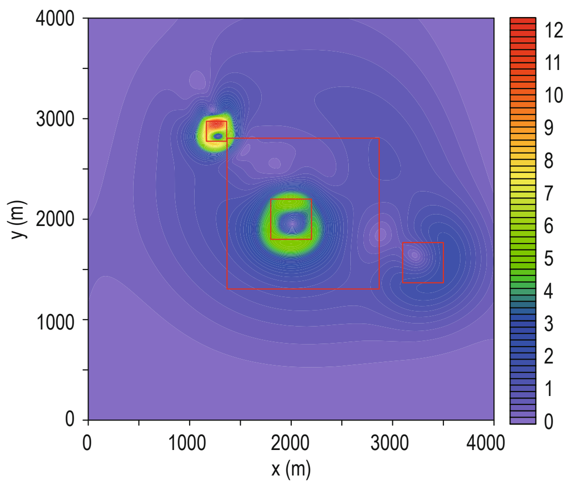

Fig.13 Contours of horizontal gradient module of gradient data after RTP at I = 40°.

Analysis using real data

To carry out application and interpretation of gradient data, a three-axis airborne magnetic gradient survey was conducted in an area in North China. The survey area is farmland region that stands relatively high in the west at 50–408 m above sea level, and low in the center and east at 17–50 m above sea level. The landforms are quite gentle. The flying altitude was 200 m. The line direction of the survey flight was due to N–S. The survey scale of the area was 1:25000. To allow future adjustment of gradient data, cross-line flying was performed in the SW direction with a cross-line interval of 1000 m. To eliminate the effect of diurnal variation in the total field, observation of the geomagnetic diurnal variation was carried out inside the survey area. Thus, traverse gradient, longitudinal gradient, vertical gradient, and total-field data were obtained.

Figure 14 shows the contour map constructed using the measured vertical gradients. Figure 15 shows the contour map from the measured vertical gradient data after RTP. RTP theory states that horizontal and vertical gradient data is the same, therefore the maps have no display. Comparing Figure 14 with Figure 15, the boundaries of the geological body lie markedly to the north after RTP that is closer to the actual boundary location. After theoretical model studies we know that the measured gradient data and total-field data that use the total gradient module method do not need RTP processing.

RTP aeromagnetic gradient data

Figure 16 shows the effect of using the total gradient module method directly on the measured gradient data, and the position of the geological boundary location is consistent with Figure 15. This suggests that the measured gradient data using the total gradient module method can delineate the central position without RTP. Some apparent anomalies in Figure 15 cannot be seen in Figure 16 and vice versa. This is mainly due to the follow: first, the vertical gradient change rate is too small, leading to a small total gradient module anomaly; second, the deep geological body is more defined on the vertical gradient contour map than on the total gradient module contour map; third, the total gradient module calculation process creates some interference. So it is feasible to determine the boundary of a shallowly buried anomaly which shows a major change rate of gradient using the total gradient module contour map. It should be noted that if the measured gradient data is not processed with RTP, the position of total gradient module contour map's maximum value is not the real central position of the geological body, it needs the conclusion of the theoretical model to determine the position.

To determine the boundaries of a geological body, the horizontal gradient module contour map is better than the total gradient module method. Figure 17 shows the horizontal gradient module contour map of measured gradient data after RTP and some boundaries of geological body can be seen. According to the theoretical model studies, the boundary position of the horizontal gradient module contour map is to the south, but the range is not very clear and it only reflects a shallow-buried geological body that has a major gradient change. Relatively speaking, the horizontal gradient module method after RTP is better and is consistent with the conclusion of the theoretical model studies.

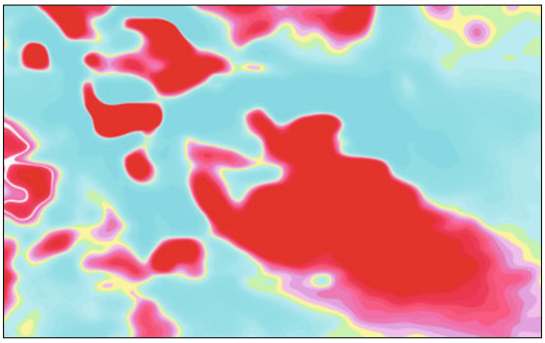

Fig.14 Contours of measured vertical gradient data.

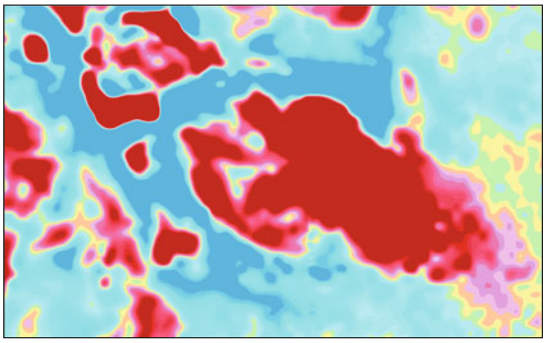

Fig.15 Contours of measured vertical gradient data after RTP.

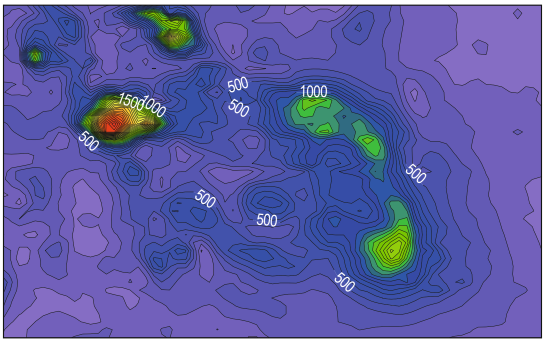

Fig.16 Contours of total gradient module of measured gradient data before RTP.

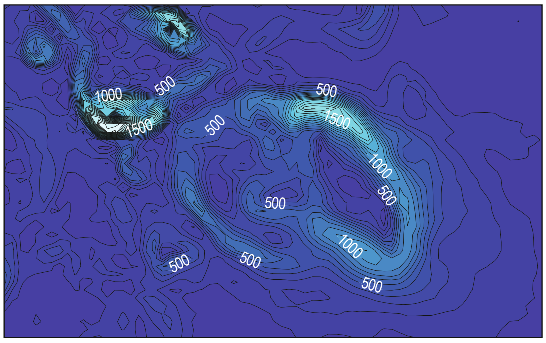

Fig.17 Contours of horizontal gradient module of measured gradient data after RTP.

Under poor RTP effects in low latitude areas, the role of the total gradient module is clear. Combined with the horizontal gradient module, it is good for determining the central and boundary positions of a shallow-buried strongly-magnetic geological body.

Conclusions

Result indicate that the RTP process is not required for gradient data or total-field data when using the total gradient module method. Therefore, we do not need to consider or measure the latitude of an area when interpreting the geology. The data used by the total gradient module method is influenced by the ambient field if no RTP process is applied, and an anomaly with a small gradient change rate is not clearly defined in the total gradient module contour map, therefore other boundary identification methods are needed. The horizontal gradient module method functions well in extracting the boundary of a geological body but it needs the RTP process, and the inclination restriction of the geomagnetic field is 20°. Therefore, a variety of methods are needed for actual data processing. At the same time, it is important to note that total-field data, after the derivation process, inevitable enlarges interference, which shows the advantage of measured gradient data for geological interpretation.

References

Ansari, A. H., and Alamdar, K., 2009, Reduction to the pole of magnetic anomalies using analytic signal: World Applied Sciences Journal, **7**(4), 405−409.

Baranov, V., 1957, A new method for interpretation of aeromagnetic maps: Pseudo-gravimetric anomalies: Geophysics, **22**(2), 359−383.

Baranov, V., and Naudy, H., 1964, Numerical calculation of the formula of reduction to the magnetic pole: Geophysics, **29**(1), 67−79.

Blakely, R. J., 1996, Potential theory in gravity and magnetic applications: New York: Cambridge University Press.

Ervin, C. P., 1976, Reduction to the magnetic pole using a fast fourier series algorithm: Computers & Geosciences, **2**(2), 211−217.

Godio, A., and Piro, S., 2005, Integrated data processing for archeological magnetic surveys: Society of Exploration Geophysicists, **24**(11), 1138−1144.

Guan, Z. N., et al, 1993, Theoretical analysis and application of the important problem in magnetic prospecting: Geological Publishing House, 76−80.

Guan, Z. N., Hou, J. S., and Yao, C. L., 1996, Application of aeromagnetic gradient data in geological mapping ang metallogenetic prognosis of gold deposits: Geoscience, (in Chinese), **10**(2), 239−249.

Guan, Z. N., and Yao, C. L., 1997, Inversion of the total gradient modulus of magnetic anomaly due to dipping dike: Social Sciences Edition Journal of China University Geosciences (in Chinese), **22**(1), 81−85.

Gunn, P. J., 1975, Linear transformations of gravity and magnetic fields: Geophysical Prospecting, **23**(2), 300−312.

Hansen, R. O., and Pawlowski, R. S., 1989, Reduction to pole at low latitudes by Wiener filtering: Geophysics, **54**(12), 1607−1613.

Huang, L. P., and Guan, Z. N., 1998, The determination of magnetic causative boundaries using total gradient modules of magnetic anomalies: Journal of East China Geological Institute (in Chinese), **21**(2), 143–150.

Keating, P., and Zerbo, L., 1996, An improved technique for reduction to the pole at low latitudes: Geophysics, **61**(1), 131−137.

Li, X. L., and Chang, S. S., 2009, Aeromagnetic gradient survey and elementary application in sandstone type uranium deposits prospecting: Uranium Geology (in Chinese), **25**(6), 355−360.

Li, Y. Y., and Yang, Y. S., 2009, Derivative-based normalized standard deviation of potential field data in geological contact mapping: Geological Science and Technology Information (in Chinese), **28**(5), 138−142.

Lin, X. X., and Ping, W., 2012, An improved method for reduction to the pole of magnetic field at low latitude —the method of frequency conversion bidirectional damping factor: Chinese Journal of Geophysics (in Chinese), **55**(10), 3477−3484.

Liu, J. X., Hu, H. J., Liu, C. M., Han, S. L., and Xie, X., 2006, Application of synthetical geophysical method on exploration of deep-seated resources: Geology and Exploration (in Chinese), **42**(4), 71−74.

Nabighian, M. N., 1972, The analytic signal of two-dimensional magnetic bodies with polygonal cross-section: Its properties and use for automated anomaly interpretation: Geophysics, **37**(3), 507−517.

Pedersen, L. B., and Rasmussen, T. M., 1990, The gradient tensor of potential field anomalies; some implications on data collection and data processing of maps: Geophysics, **55**(12), 1558−1566.

Peter, H., 1986, The application of aeromagnetic gradient survey method for prospecting gold deposits in Quebec Waerdeao mining area: Foreign Geoexploration Technology (in Chinese), 31−36.

Qi, M., Zhang, B. L., Fu, C., et al, 2009, Fast discovery of concealed Cu-W polymetallic deposit in central inner Monggulia by applying comprehensive exploration methods: Geology and Exploration (in Chinese), **45**(6), 676−682.

Silva, J. B. C., 1986, Reduction to the pole as an inverse problem and its application to low-latitude anomalies: Geophysics, **51**(2), 369−382.

Sun, Y. M., Li, Q. X., Xu, H. P., et al., 1995, Image processing and programming of data conversion in the geophysical data field: Jilin Science&Technology Press, Changchun, China, 10–78.

Wang, J. R., and Sun, L. C., 1990, The application of resistivity medium gradient method to the exploration of ground cracks in Xi'an: Geophysical and Geochemical Exploration (in Chinese), **14**(6), 473–476.

Wu, W. X., Fan, W. Y., and Wang, Y. H., 2013, Determination of the magnetic source boundary based on total gradient module analysis and its prospecting significance: Geology and Exploration (in Chinese), **49**(6), 1164–1169.

Xian, J. A., Guo, Y. F., Liang, K. J., and Chen, K. D., 2013, Difference of the measured 3-dimension ΔT gradient of air magnetic survey and conversion of the 3-dimension ΔT gradient: Contributions to Geology and Mineral Resources Research (in Chinese), **28**(2), 297–300.

Zhang, C. D., 2006, Airborne tensor magnetic gradiometry-the latest progress of airborne magnetometric technology: Chinese Journal of Engineering Geophysics (in Chinese), **3**(5), 354–361.

Li Lin, graduated from College of GeoExploration Sicence and Technology of Jilin University in 2011 and obtained bachelor's degree. Graduated from College of Geo Exploration Sicence and Technology of Jilin University in 2014 and obtained master's degree. Now in the college study for a doctorate. The main research interest is the gravity and magnetic potential field data processing and interpretation.